The Biophysical Properties of Microalgal Cell Surfaces Govern Their Interactions with an Amphiphilic Chitosan Derivative Used for Flocculation and Flotation

Irem Demir-Yilmaz, Michaela Pappa, Sanjaya Lama, Pascal Guiraud, Dries Vandamme, Cécile Formosa-Dague

The biophysical properties of microalgal cell surfaces govern their interactions with an amphiphilic chitosan derivative used for flocculation and flotation

Irem Demir-Yilmaz[1], Michaela Pappa[2], Sanjaya Lama[2], Pascal Guiraud[1], Dries Vandamme[2] and Cécile Formosa-Dague[1*]

[1] TBI, Université de Toulouse, INSA, INRAE, CNRS, 31 400 Toulouse, France.

[2] Analytical and Circular Chemistry, Institute for Material Research, Hasselt University, 3590 Diepenbeek, Belgium

*corresponding author: Cécile Formosa-Dague, formosa@insa-toulouse.fr

Postal address: Toulouse Biotechnology Institute, INSA de Toulouse, 135 avenue de Rangueil, 31077 Toulouse Cedex 4, France

Phone : + 33 5 61 55 99 67

ABSTRACT (300 words)

Microalgae show great promise for producing valuable molecules like biofuels, but their large-scale production faces challenges, with harvesting being particularly expensive due to their low concentration in water, necessitating extensive treatment. While methods like centrifugation and filtration have been proposed, their efficiency and cost-effectiveness are limited. Flotation, involving air-bubbles lifting microalgae to the surface, offers a viable alternative, yet the repulsive interaction between bubbles and cells can hinder its effectiveness. Previous research from our group proposed using an amphiphilic chitosan derivative, poly-octyl chitosan (PO-chitosan), to functionalize bubbles used in dissolved air flotation (DAF). Molecular-scale studies performed using atomic force microscopy (AFM) revealed that PO-chitosan's efficiency correlates with cell surface properties, particularly hydrophobic ones, raising the question of whether this molecule can in fact be used more generally to harvest different microalgae. Evaluating this, we used a different strain of *C. vulgaris* and first characterized its surface properties using AFM. Results showed that cells were hydrophilic, but could still interact with PO-chitosan on bubble surfaces through a different mechanism based on specific interactions. Although force levels were low, flotation resulted in 84% of separation, which could be explained by the presence of AOM (algal organic matter) that also interact with functionalized bubbles, enhancing the overall separation. Finally, flocculation was also shown to be efficient and pH-independent, demonstrating the potential of PO-chitosan for harvesting microalgae with different cell surface properties and thus for further sustainable large-scale applications.

KEYWORDS

Chlorella vulgaris, Hydrophobicity, Flocculation, Flotation, Algal Organic Matter, Force Spectroscopy

INTRODUCTION

Microalgae, photosynthetic microorganisms, offer significant potential in various fields due to their ability to convert sunlight and carbon dioxide into valuable products. While the most significant application of microalgae lies in biofuels production, microalgae are also a rich source of proteins, essential fatty acids, vitamins and other nutrients, making them good candidates for nutritious foods or animal feed[1]. In comparison to terrestrial plants, microalgae offer numerous advantages. They can be cultivated year-round[2], require less water than terrestrial crops despite growing in aqueous environments[3], and can utilize nutrients present in wastewater for their cultivation[4]. Additionally, their cultivation does not necessitate the use of herbicides or pesticides, and their rapid growth rate (microalgae can achieve a yield 10 to 20 times higher than oil palm) and high oil production (compared to soybean, microalgae can produce up to 300 times more of oil)[5] make them particularly promising for biofuel applications, surpassing traditional terrestrial plants in efficiency. However, the widespread adoption of microalgae-based biodiesel faces hurdles due to the costly production process[6], which involves cultivation, harvesting, and biorefining[7]. Among these steps, harvesting is the most expensive, especially considering that microalgae typically grow in low concentrations in water (0.3–3 g/L), requiring significant water treatment efforts due to the large volumes involved[8].

Several techniques have been proposed for microalgae separation, the most commonly used in industrial processes being centrifugation and filtration, even though these approaches are associated with significant operational expenses and energy consumption[9,10]. In this context, flotation is a good alternative, which consists of generating rising air-bubbles in a microalgae suspension. As a consequence, microalgae cells attach to bubbles and are transported to the surface without being damaged[11]. Yet, the effectiveness of this method may be hindered by the repulsive interaction between bubbles and cells, which arises from the negative surface charge of both cells and bubbles in water, coupled with the limited hydrophobicity of microalgae. In order to make this technique efficient for harvesting microalgae, a first possibility is to add a flocculation step prior to flotation. Typically, the natural tendency for microalgal cells to aggregate in suspension is inhibited by the negative surface charge characteristic of most microalgae species[12]. Hence, positively-charged flocculants are commonly introduced into the algal suspension to aggregate cells into larger flocs, increasing their likelihood of being captured by ascending air bubbles[13]. However, synthetic flocculants are frequently used, posing the risk of contaminating both the harvested biomass and subsequent stages of processing, including recycled water[14]. For these reasons, using bio-sourced polymers as flocculants is an interesting alternative. Such flocculants have different advantages; they are non-toxic, biodegradable, relatively cheap and can be abundantly available in nature[15,16]. As an example, chitosan is derived from the deacetylation of chitin found in shrimp. It acts as a polyelectrolyte and becomes positively charged at pH levels below its pKa (6.5). After cellulose, it stands as one of the most prevalent natural polymers on the planet[17]. Because of these advantages, it has been widely used to flocculate different microalgae species in a pH dependent manner. In a recent work from our team, we used atomic force microscopy (AFM) to access the interactions between chitosan and the cell surface *Chlorella vulgaris* (strain CCAP 211/B11) at the molecular scale[18], and found that in fact the chitosan induced flocculation mechanism is different depending on the pH. At low pH (≤6), it is based on specific interactions between the flocculant and macromolecules present on the cell surface. Yet, at higher pH (at pH 8), chitosan precipitates and flocculates cells through a sweeping mechanism[19]. Because of the interest/applicability of this molecule, many studies have attempted to modify it in order to increase its possibilities. For example, our group has recently modified chitosan with hydrophobic groups, which resulted in higher flocculation efficiencies using *C. vulgaris* in a wider range of pH. AFM experiments in this case showed that in fact the flocculation mechanism was different from chitosan, as the interaction between this modified

chitosan molecule, called poly-octyl chitosan (PO-chitosan), was based on hydrophobic interactions with the cell surface[20].

Another alternative for increasing flotation efficiency is to modify the bubble surface with a molecule that will interact with cells, allowing to achieve efficient separation without the need of a flocculation step. This concept was first used for microalgae harvesting in 2008 by the team of Henderson[21,22]. In the strategy developed by this team, bubbles were functionalized with cationic polymers, making their surface positively charged. These modified bubbles could then attract microalgae cells, which typically carry a negative charge, through electrostatic forces, facilitating their capture and subsequent separation[21–23]. Recently, our group advanced this concept by functionalizing bubble surfaces with PO-chitosan, with the aim of attracting cells thanks to specific interactions between bubbles and cells instead of electrostatic ones[20]. In particular, in this work, we used a combination of AFM with microfluidics (FluidFM[24]) to produce functionalized micro-sized bubbles and measure their interactions at the molecular level with cells, using recent developments of our team[25]. These experiments allowed us to show that the functionalization of bubbles with PO-chitosan allowed increasing significantly their interactions with *C. vulgaris* cells (CCAP strain 211/11B) in a pH-dependent manner. However, the force curves obtained showed that hydrophobicity was the dominant component of the interaction between cells and functionalized bubbles, possibly because this particular *C. vulgaris* strain present hydrophobic properties, and probably hiding the first and expected specific interaction between the chitosan backbone on the bubble surface and cells. Interestingly, additional flotation tests revealed a direct correlation between the efficiency of flotation achieved with modified bubbles and the adhesion forces measured between cells and these treated bubbles. This suggested that greater adhesion forces lead to improved separation efficiencies during the flotation process[20]. In the best conditions, the separation efficiency doubled with PO-chitosan bubbles, demonstrating the efficiency of this flotation process[20].

Thus, our previous results showed the potential of PO-chitosan to efficiently separate *C. vulgaris* cells (strain CCAP 211/11B) from their culture medium by using it either as a flocculant, or as a surfactant to functionalize bubbles and perform separation through a one-step flotation process. But as we also showed, the efficiency of the molecule is directly correlated to the cell surface properties, especially hydrophobic properties, which raises the question to know if this molecule can in fact be used more generally to harvest microalgae cells with different surface properties. In that regard, *C. vulgaris* is an interesting species with many different strains that show a wide variety of cell wall matrices. For instance, Gerken *et al.* found that 10 different strains of *C. vulgaris* reacted differently to the same enzymatic cocktails, illustrating the fact that all 10 strains had different cell wall polysaccharidic compositions and/or architecture[26]. Such differences can be due to the fact that cells adapt to the habitat they live in, so depending on where the strains were isolated, their cell wall present different properties, which can have important impacts on the physico-chemical properties of the cell surface (notably hydrophilic/hydrophobic properties). Moreover, various strains of the same species may exhibit variations in the composition of the algal organic matter they generate, which can significantly impact both flocculation and flotation processes[27]. Thus in this work, we investigated the potential of PO-chitosan to interact with the cell wall of a different *C. vulgaris* strain, thereafter named strain F010102-A, isolated in Cuba in 2002[28]. After characterizing the cell wall properties of this strain using AFM, we then show how it interacts with PO-chitosan used either as a flocculant or present at the surface of bubbles, and the consequences on both types of separation processes at the population scale.

Moreover, we also investigate the role of algal organic matter (AOM) in the interactions with functionalized bubbles to assess their potential role in the separation. Altogether, this work enhances our understanding of the PO-chitosan interactions with cell surfaces, and show that it can become a generic molecule to harvest different microalgae species with different cell surface properties.

MATERIALS AND METHODS

Microalgae strain and culture. The freshwater green microalga *Chlorella vulgaris* strain F010102-A from the Universidad de Oriente, Cuba[28], was cultivated in BG-11 medium prepared with sterilized deionized water. Cells were cultivated in bubble column photobioreactors (30 L, Length × Diameter: 100 cm × 20 cm) at room temperature (20 ± 2°C). The system was mixed by sparging with 0.2 µm filtered air (2 L.min^{-1}) and the pH was controlled at 8.5 by addition of 2–3 % pure CO_2 using a pH-controller system. The photobioreactor culture was irradiated (16:8 h light: dark cycle) on two opposite sides with LED lights (7000K- daylight, 4000K- warm white, and RGB colored 1200 mm GoldLine LED, HVP Aqua) producing a photon flux density of approximately 150 µmol·photons·m^{-2}·s^{-1} at the surface of the reactor. Microalgal culture growth was monitored by measuring optical density at 750 nm (OD_{750}) using a UV-visible spectrophotometer (Ultraspec-7000). Absorbance was calibrated against microalgal dry weight concentration, which was determined gravimetrically by filtering a known volume of culture on pre-weighed glass microfiber filters (Whatman GF6, 47 mm diameter) and drying overnight at 105°C.

For AFM experiments, cells were inoculated in small culture flasks of 50 mL and incubated for 6 days (exponential phase) at 20 °C, in an incubator equipped with white neon light tubes (illumination of 40 µmol·photons·m^{-2}·s^{-1}), under 120 rpm agitation, with a photoperiod of 18 h light 6 h dark. Before AFM experiments, cells were harvested by centrifugation (3000 rpm, 3 min), washed two times in PBS at pH 8, and immobilized on positively charged glass slides (Superfrost™ Plus adhesion, Epredia, USA), following the procedure described in [29]. AFM experiments were performed in PBS buffer at pH 8 to mimic the culture medium pH at the end of the 6-days cultures used unless stated otherwise.

Synthesis of PO-Chitosan. The PO-chitosan (N-octyl-chitosan derivatives) used in this study was synthesized using a reductive amination reaction as described in Demir-Yilmaz *et al*. 2023[20]. Briefly, high molecular weight chitosan (from shrimp, practical grade, ≥ 75% degree of deacetylation, Sigma-Aldrich reference C3646) was dissolved in 0.2M acetic acid (AcOH) and ethanol was added after complete dissolution. The pH was adjusted to 6 with NaOH to prevent macromolecule precipitation. Then, a solution of octanal in 40% ethanol was added to the chitosan solution using a 1:3 ratio prior to adding an excess of sodium cyanoborohydride (NaBH$_3$CN). The acetylation degree of the resulting molecule was determined to be 12% using NMR spectroscopy as described elsewhere[20]. To perform experiments, PO-chitosan was dissolved in water with overnight stirring and the addition of 2M acetic acid to decrease the pH. The complete dissolution of the PO-chitosan was measured as described in [20] using granulometry and turbidity measurements.

Roughness analyses. High resolution (512 lines), 1 x 1 µm, images were recorded on top of cells using a Nanowizard IV AFM (Bruker, USA), in contact mode using MSCT cantilevers (Bruker, nominal spring constant of 0.01 N/m). For each condition, 12 cells coming from at least 2 independent cultures were

imaged using an applied force < 1 nN. For these experiments, the cantilevers spring constants were determined by the thermal noise method prior to imaging[30]. To determine the arithmetic average roughness (Ra), the height images recorded were treated using the Data Processing software (Bruker, USA).

Nanomechanical analyses. Nanoindentation experiments were performed in force spectroscopy mode (applied force of 2.5 nN) with MSCT cantilevers (Bruker, nominal spring constant of 0.01 N/m). For each condition, 12 cells coming from at least 2 independent cultures were analyzed (approximately 400 force curves were recorded for each cell). Young's moduli were then calculated from 50 nm long indentation curves using the Hertz model. In this model, the force F, the indentation (δ), and the Young's modulus (Ym) follow equation 1, where α is the tip opening angle (17.5°), and υ the Poisson ratio (arbitrarily assumed to be 0.5). The cantilevers spring constants were determined by the thermal noise method [30].

$$F = \frac{2 \times Ym \times \tan\alpha}{\pi \times (1 - \upsilon^2) \times \delta^2} \qquad (1)$$

Flocculation and flotation experiments. Flocculation jar tests were performed on mid-exponential phase culture with a biomass concentration of ~0.3 g·L^{-1} (corresponding to an OD$_{750}$ of ~0.867–0.918). To a series of plastic jars (each containing 100 mL of culture), flocculant PO-chitosan was directly added to have a final concentration of 20, 25 and 30 mg/L. During addition of the flocculant, the culture suspensions were stirred at 200 rpm using a multi-position magnetic stirrer (IKA RO 15) for 20 minutes and left to settle for 30 minutes. 3.5 mL of sample was taken from the middle of the clarified suspension to measure OD$_{750}$ and subsequently to determine the flocculation efficiency.

Flotation experiments were performed in Platypus DAF jar tester (Aquagenics Pty Ltd, Australia), following a procedure described in [31]. In summary, 1 L of cells at mid-exponential growth phase, with an initial OD$_{750}$ of 1, was added to test jars. Water containing varying concentrations of PO-chitosan (30, 25, and 20 mg/L) was introduced into a pressurization tank and pressurized at 6 bars for 10 minutes. Following this, depressurization allowed for the injection of functionalized microbubbles into flotation beakers (with bubble volumes of 200, 350, and 500 mL), and 200 mL of algal suspension was sampled from the test jars to assess flotation efficiency.

In both sets of experiments (flocculation and flotation), the optical density of the withdrawn microalgae suspension (ODf) was measured and compared with the initial optical density of the microalgae suspension before the experiments (ODi), while also factoring in the initial and final volumes (Vi and Vf). Flotation efficiency (E) was then determined using Equation 2.

$$E = \frac{OD_i.V_i - OD_f.V_f}{OD_i.V_i} \qquad (2)$$

Zeta Potential measurement. Aliquots from the clarified part of the suspension were taken as is and measured for their electrophoretic mobility with the Zetasizer Nano (Malvern, UK) with the DTS1070 disposable cuvettes (Sysmex Europe, Germany).

Hydrophobicity measurement with bubble probe method using FluidFM. Air-bubbles were formed using a Nanowizard IV AFM (Bruker, USA), equipped with FluidFM technology (Cytosurge AG,

Switzerland), following the same procedure described in Demir *et al.* [25], in PBS buffer at pH 8. Interactions between these bubbles and single *C. vulgaris* strain F010102-A cells were recorded using an applied force of 1 nN, a z-range of up to 2 µm and a constant retraction speed up to 4 µm/s. The measurements were performed using 10 different cells coming from at least two independent cultures.

Bubble functionalization. PO-chitosan functionalized bubbles were produced following the procedure described elsewhere[20,25], using a 2 mg/L PO-chitosan solution. Interactions between PO-chitosan coated bubbles and single *C. vulgaris* strain F010102-A cells were recorded at pH 8 using an applied force of 1 nN, a z-range of up to 2 µm and a constant retraction speed up to 2 µm/s. The measurements were performed using 8 different cells coming from at least two independent cultures.

Single-cell force spectroscopy experiments. Force spectroscopy experiments were conducted using a NanoWizard IV AFM (Bruker, USA), in PBS buffer, using triangular tipless NP-O10 probes (Bruker, USA, nominal spring constant of 0.06 N/m). AFM cantilevers were functionalized with single *C. vulgaris* strain F010102-A cells using the same procedure described in [19]. The cell probes produced were then used to measure interactions with PO-chitosan and chitosan-functionalized glass slides. Both molecules were functionalized at the surface of glass-slides using spin-coating, according to procedures described in [19,20]. Interactions between single *C. vulgaris* strain F010102-A cells and both initial chitosan (at pH 6) and PO-chitosan (at pH 8) were recorded using an applied force of 1 nN, a z-range of up to 2 µm and a constant retraction speed comprised between 2.0 and 4 µm/s. The force curves acquired were treated using the Data Processing software provided by Bruker to obtain the maximum adhesion force on each retract curves. The measurements were performed using 8 different cells coming from at least two independent cultures.

Isolation and ultrafiltration of extracellular soluble algal organic matter (AOM). AOM from exponential phase (day 6) culture of *C. vulgaris* strain F010102-A were isolated following the procedures described in [32]. Briefly, the extracellular soluble organic matter was separated from the culture by continuous centrifugation at 8000 rpm (FJ 130 EPR, Milky Day, Czech Republic). The supernatant obtained was centrifuged 3 to 4 times until it was free of cells. Thus, obtained cell/debris free culture supernatant is referred to as extracellular soluble algal organic matter (AOM). Ultrafiltration and diafiltration of isolated AOM were carried out using a tangential flow filtration system (ÄKTA flux 6, Cytiva) equipped with a Xampler hollowfiber cartridge (UFP-50-C-4X2MA, Cytiva) with a pore size of nominal molecular weight cut-off (NMWCO) of 50 kDa. Ultrafiltration was operated at constant transmembrane pressure (TMP) of 0.6 bar in retentate recycle mode to concentrate feed AOM solution ~24 fold [33,34]. Diafiltration was performed with distilled water till the permeate conductivity was reduced from an initial value of 650 µS/cm to a final value of less than 20 µS/cm. Thus, obtained concentrated (ultra-filtered/dia-filtered) AOM fraction larger than 50 kDa (hereafter referred to as AOM concentrate) was collected and lyophilized for 24 h at -40°C under 0.12 mbar vacuum pressure (CHRIST, ALPHA 1-2 LDPlus) resulting in lyophilized AOM concentrate yield of 0.12 g/L. The AOM concentrate was stored in the airtight vial at -20°C until further use.

AOM concentrate immobilization. AOM concentrate immobilization was performed using a previously described method [35]. In short, 1 mL of AOM concentrate solution (24 mg/L) was deposited on polystyrene (PS) petri-dish and incubated for 4 days at 4°C to allow adsorption of AOM on the PS

surface. Before the experiments, the petri-dish was then incubated for 30 min in the room temperature to warm up. Then petri-dish was carefully washed with PBS buffer to remove non-attached AOM. These AOM surfaces were then used in force spectroscopy experiments to measure the interactions with clean bubbles formed as previously described.

Statistical analysis. The experimental findings are presented as the mean ± standard deviation (SD) from a minimum of three replicates, with the specific number of replicates noted in the Results and Discussion section. Student's t-test was employed to evaluate differences in results for large samples, while the Mann-Whitney test was used for smaller samples (less than 20). Significance was determined at $p < 0.05$.

RESULTS AND DISCUSSION

AFM characterization of the biophysical properties of *C. vulgaris* strain F010102-A cell surface

The microalgae *C. vulgaris* strain F010102-A used in this study was isolated from the aquaculture station of Maffo, Contramaestre in Cuba. Because the CCAP strain used in our previous study was isolated in the Netherlands, it is likely that it will have different cell surface properties. Thus, in a first step, the surface properties of *C. vulgaris* strain F010102-A cells were characterized and compared with the CCAP strain for which the PO-chitosan functionalized bubbles flotation process was initially developed. The cell surface represents the interface with which bubbles will interact. For that, first, cells were imaged using AFM in quantitative imaging mode (QI), as shown in Figure 1a. As can be seen on the image, cells have a round shape, as expected, and do not show differences with the CCAP *C. vulgaris* strain used in our first study. We then took a closer look at the cell surface and conducted high resolution contact images on small areas on top of cells (1 µm x 1 µm). An example of such zoom-in height image is presented in Figure 1b. The cross section (Figure 1b) taking along the white line shows large and wide pattern between -5 to 15 nm on a large distance of 200 nm (Figure 1c), suggesting that the surface is rather rough. Hence, the average roughness Ra of the surface was quantified and showed that *C. vulgaris* strain F010102-A cells have an average roughness of 2.1 ± 0.5 nm (Table S1, the error corresponds to the standard error of the mean). The average roughness is slightly higher than the *C. vulgaris* CCAP cells (1.7 ± 0.9 nm) at the same pH of 8[19], but is not significantly different, indicating that the surface nanomorphology of both strains is similar.

Although the cell surface structures may appear similar, variations in cell wall composition and architecture, specifically how different components are arranged within the cell wall, can result in differing nanomechanical properties. Thus, the Young's modulus (Ym) of the microalgae cell wall was determined through nanoindentation measurements performed on areas of 1 µm × 1 µm on top of cells. Figure 1d shows the distribution of Ym values obtained on 12 cells (coming from 2 independent cultures, n = 4749 force curves) showing that the average Ym is 1488.9 ± 408.8 kPa (full data are presented in Table S1, the error corresponds to the standard error of the mean). Compared to the *C. vulgaris* CCAP strain for which the average Ym was of 981.6 ± 554.4 kPa at the same pH of 8[19], this value is significantly higher, meaning that *C. vulgaris* strain F010102-A cells are thus more rigid, which could be due to a different cell wall organization, or a different cell wall composition[36].

Lastly, the hydrophobic properties of *C. vulgaris* strain F010102-A cells were evaluated. For that, the bubble probe method developed in our team[25] was employed. This technique involves using FluidFM to create a bubble at the opening of a microfluidic cantilever and probing the interactions between this bubble, a hydrophobic interface in water, and cells immobilized on a surface (Figure 1e). The distribution of the adhesion forces obtained is presented in Figure 1f. On all cells probed, the retract force curves recorded do not show any adhesions at pH 8 (inset on Figure 1f), meaning that there are no interactions at all between cells and the bubble probe, and that the cell surface is completely hydrophilic. In the case of the CCAP strain, at the same pH, the force curves recorded with clean bubbles showed adhesions with an average force of 1.3 ± 0.6 nN (Figure S1), showing that cells had hydrophobic properties at this pH.

To conclude, these AFM experiments showed that cells of the strain F010102-A have a similar cell surface structure compared to the CCAP strain cells, illustrated by a similar roughness recorded. However, despite this similar structure, the nanomechanical measurements performed showed that the

two strains have a different cell wall composition and/or architecture, with strain F010102-A cells being significantly more rigid. Finally, the measurement of the hydrophobic properties of cells showed that at a pH of 8, cells of the strain F010102-A are completely hydrophilic, while it was not the case with cells of the CCAP strain. This difference further confirms that the two strains have most likely a different cell wall composition, but is also an important point as because of this, cells of the strain F010102-A will not be able to establish hydrophobic interactions with PO-chitosan used either as a flocculant or on bubble surface. Yet, for the CCAP strain, we had shown in our previous study that it was thanks to hydrophobic interactions that cells could interact with the molecule, thus enabling their separation at the population
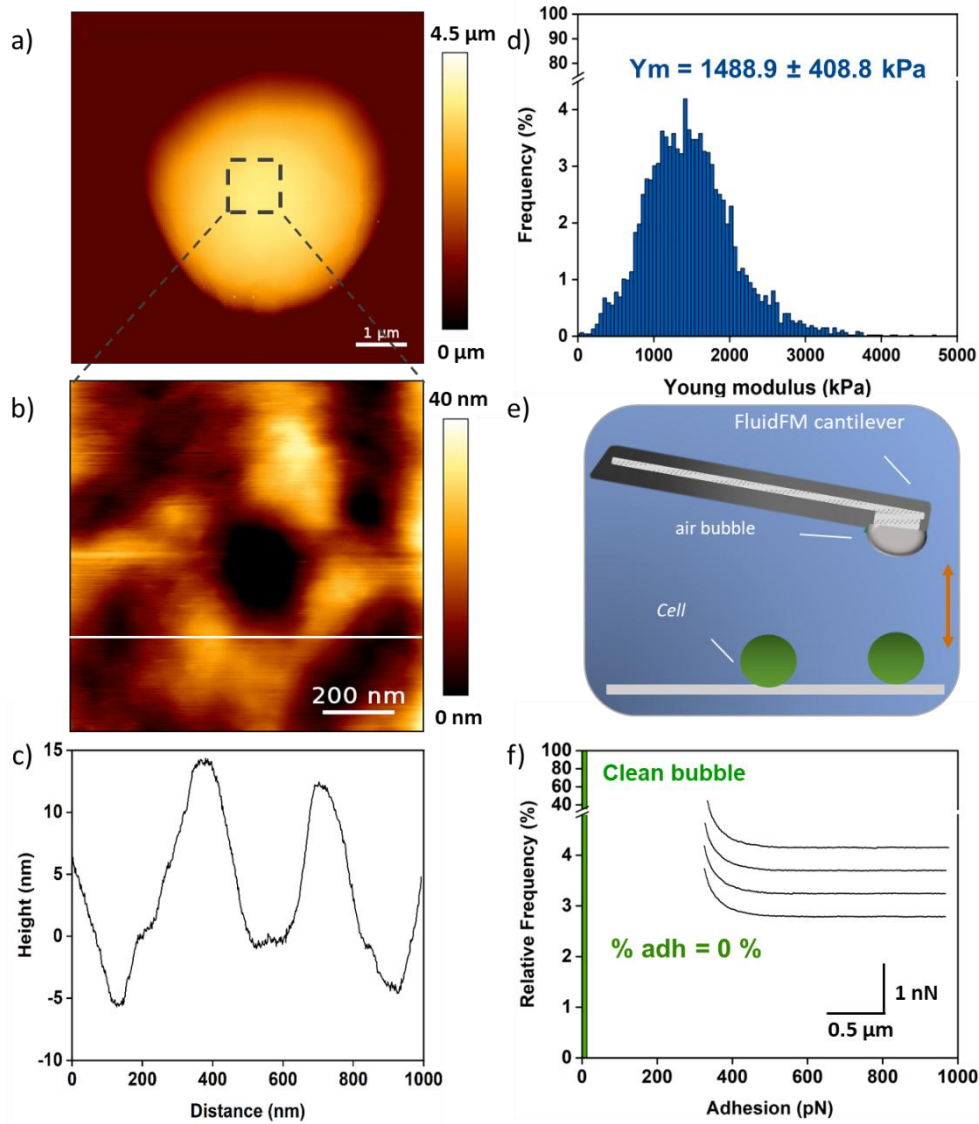
scale.

Figure 1: Biophysical properties of C. vulgaris strain F010102-A cell surface. *a) AFM height image of a whole cell immobilized on a positively-charged surface. b) AFM height image recorded on an area of 1 μm x 1 μm on top of a cell. c) Cross-section taken along the white line in b. d) Histogram showing the distribution of Young modulus values for 12 cells. e) Schematic representation of hydrophobicity*

measurements performed with the bubble probe method. f) Adhesion force histogram obtained between bubble and C. vulgaris strain F010102-A cells.

PO-functionalized bubbles interact with cells through a different adhesion mechanism

In a next step, we then assessed if the hydrophilic character of the *C. vulgaris* strain F010102-A cells could prevent them from interacting with PO-chitosan functionalized bubbles. For that we used FluidFM to produce functionalized bubbles with PO-chitosan (2 mg/L) and probe their interactions with individual cells (Figure 2a). When performing these experiments with cells of the strain F010102-A, the obtained retract force curves show multiple binding events (inset in Figure 2b) with an average adhesion force of 316.9 ± 215.9 pN (n = 2810 force curves from 8 cells coming from 2 independent cultures). The range of adhesion forces (Figure 2b) and the observed force patterns align with the unfolding of elongated macromolecules from the surface of the cell[37,38]. Here note that a large standard deviation resulting from the wide distribution of the adhesion values can be observed, which is caused by the heterogeneity of the living cells. These results indicate that *C. vulgaris* strain F010102-A cells are able to interact with bubbles when they are functionalized with PO-chitosan while it was not the case with clean bubbles, indicating that the flotation process might be efficient to harvest cells at the population scale.

In our previous study in the case of the CCAP strain, the interactions with functionalized bubbles resulted in much higher adhesion forces (13 nN), and no molecular unfoldings were observed on the force curves, only one peak at the contact point resulting from the dominant hydrophobic interaction between cells and bubbles[20]. To understand the differences between the two *C. vulgaris* strains, it is important to understand what part of the PO-chitosan molecule is exposed at the surface of bubbles. Basically, surfactants like PO-chitosan are absorbed on the bubble surface in a way that hydrophobic parts of the molecule stay inside of the bubble whereas the hydrophilic chitosan backbone is exposed on the bubble surface, as shown in Figure 2c. Since cells of the strain F010102-A cannot establish a hydrophobic interaction with the bubble as they are hydrophilic, the unfoldings that we observe on the force curves most likely result from the interaction between the cell surface and the chitosan backbone at the surface of bubbles. If we compare these results to the ones obtained when probing the interactions between strain CCAP cells and chitosan surfaces[19], the unfoldings patterns are similar, as well as the adhesion forces obtained (around 300 pN), indicating that most likely a similar specific interaction takes place here. Interestingly, a repulsion between the cell and the clean bubble surface can be directly observed on the approach curves obtained, starting at a distance of approximately 200 nm (Figure 2d). This can be explained by the fact that both cells (zeta potential of -41.32 ±1.39 mV) and clean bubbles are negatively-charged in water[39]. However when bubbles are functionalized, this repulsion is not visible anymore, indicating that most probably the charge of the bubble has changed with the presence of the chitosan backbone at its surface, which should be positively-charged at the pH considered (zeta potential of + 10 mV[40]).
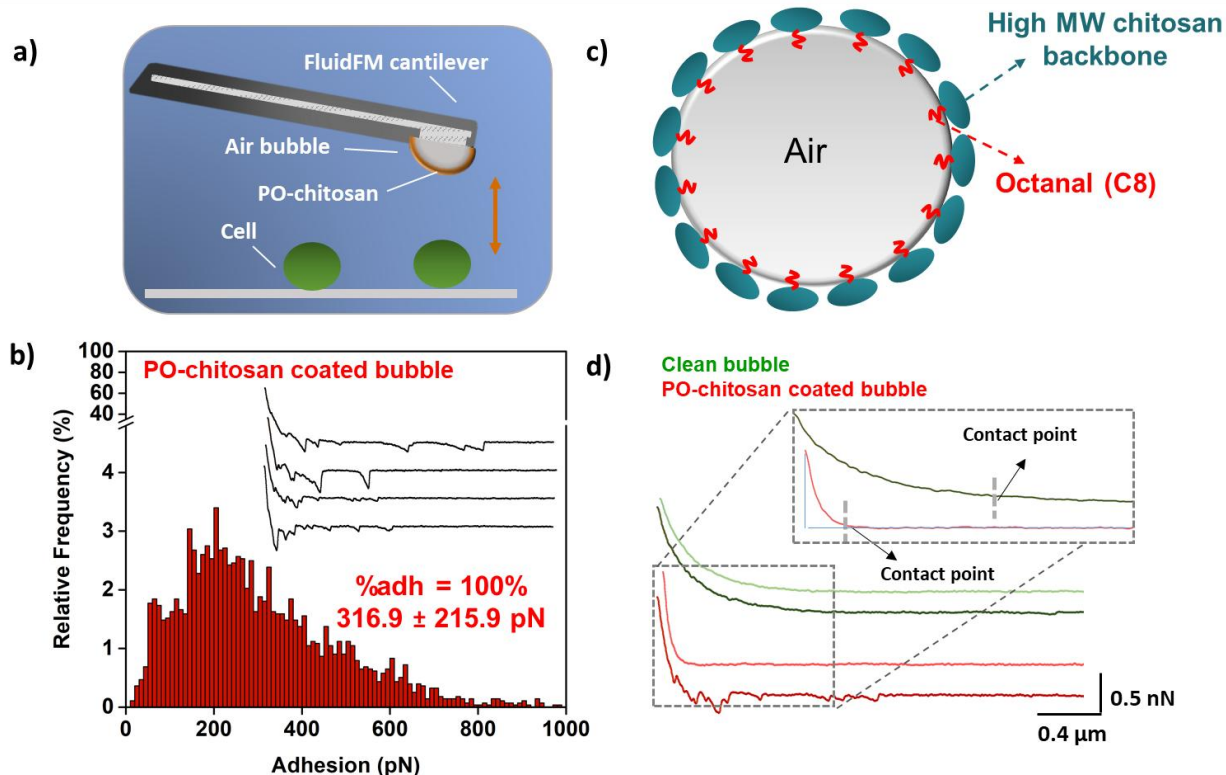
Figure 2. Modulation of bubble cell interaction with PO-chitosan functionalize bubble. *a) Schematic representation of the force spectroscopy experiments performed. b) histogram showing the distribution of the adhesion values obtained at pH 8. c) Schematic representation of the organization of PO-chitosan molecules at the surface of bubbles. d) Representative force curves obtained for PO-chitosan coated bubble-cells and clean bubble-cell interactions at pH 8.*

Subsequently, single-cell force spectroscopy experiments were performed to validate that the cell surface of the *C. vulgaris* strain F010102-A interacts through specific interactions with the chitosan backbone of PO-chitosan present at the surface of bubbles. In these experiments, individual cells are attached to tipless cantilevers and used to probe the interactions with surfaces coated with chitosan (Figure S2) which mimic the surface of the PO-chitosan functionalized bubbles. Note that in this case, the experiments were performed at a pH of 6 as chitosan precipitates at higher pH[19,40]. The retract force curves obtained show this case multiple binding events reflecting unfolding of long macromolecules from the cell wall with an average adhesion force of 0.4 ± 0.2 nN. These unfoldings are similar to those obtained when cells interact with the surface of PO-chitosan functionalized bubbles (Figure 2b), with adhesion forces in the same range. These results thus confirm our hypothesis that cells interact specifically with the chitosan backbone present on functionalized bubbles surfaces.

PO-chitosan functionalized bubbles flotation process is efficient despite low adhesions forces between cells and bubbles.

The previous results allowed to understand that *C. vulgaris* strain F010102-A cells interact with PO-chitosan functionalized bubbles through specific interactions with the chitosan backbone exposed at the surface of bubbles. In our previous study, adhesion forces between the CCAP strain and functionalized bubbles were of 12.8 nN, which resulted in a separation efficiency of approximately 60 %. Here the mean adhesion forces recorded are approximately of 350 pN; the next question that thus

arises is to know whether these comparatively low-force adhesions are sufficient to promote an efficient capture of the cells by the functionalized bubbles during the flotation process. To answer this question, we next performed flotation experiments with functionalized bubbles; figure 3a shows the schematic representation of this flotation process. Twenty minutes after the cells and bubbles attained the surface, macroscopic optical images were taken in order to first evaluate if there is indeed an interaction between the functionalized bubbles and the cells. As it can be observed on Figure 3a, cells directly aggregate around bubbles without the need of a prior flocculation step.

Then, optimization of the flotation process was conducted by varying first the ratio of the bubble volume and cells. For that, three different white water volumes (200, 350 and 500 mL) were tested while keeping the cell suspension volume constant of 1 L. Increasing the white water volume is proportional to the bubbles surface area that can interact with the cells. The results obtained are presented in Figure 3b. On this bar chart, light green bars correspond to the control experiment (clean bubble) and dark green bars correspond to the PO-chitosan coated bubble (25 mg/L). Using clean bubbles, regardless of the bubble volume used, the separation efficiency is around 0 %, which was expected since we showed that clean bubbles do not interact with cells at all (Figure 1f), and even have a repulsive interaction (Figure 2d). However, the separation efficiencies obtained with PO-chitosan bubbles at a concentration of 25 mg/L (concentration that gave the best results in the case of *C. vulgaris* CCAP) increased to 68.6 ± 2.1 %, 84.1 ± 1.1% and 84.8 ± 0.8%, with 200, 350 and 500 mL white water volume, respectively. Basically, for a low bubble volume of 200 mL, lower separation efficiencies are obtained probably because the surface area of the bubbles is not large enough both for the cell surface and for the quantity of PO-chitosan present in the solution. For the higher bubble volumes, higher separation efficiencies were obtained, of approximately 84% in both cases. The 350 mL white water volume was chosen for the rest of the experiments since it achieves equivalent separation with lower water footprint.

Secondly, the influence of the PO-chitosan concentration used on the flotation efficiency was evaluated. For that we selected 3 different concentrations, 20, 25 and 30 mg/L of PO-chitosan with 350 mL white water volume, which resulted in separation efficiencies of 72.1 ± 0.8% , 84.1 ± 1.1% and 60.9 ± 4.5%, respectively (Figure 3c). Indeed, at low concentration, the quantity of PO-chitosan is not enough to cover the surface of bubbles, which results in decreased separation efficiency. An elevated concentration of 30 mg/L of PO-chitosan surpassed the bubble capacity, potentially leading to excess PO-chitosan molecules in the suspension. This saturation could hinder bubble-cell interactions, impeding effective flotation. In comparison, separation efficiencies obtained for the CCAP strain were approximately of 60%, so 1.4 times lower than the current strain using the same PO-chitosan concentration (25 mg/L) with a higher of bubble/cell volume ratio (50 mL of bubbles for 100 mL of cells), showing the superior efficiency of the one-step flotation process with the current strain.

To further understand these results, we then checked the zeta potential of the clarified suspensions (below the cake, see Figure S3), when clean bubbles and PO-chitosan functionalized bubbles (at the different concentrations tested, bubble volume of 350 mL) were used. These samples contain the unharvested cells along with their excreted organic matter, and possibly also free PO-chitosan molecules released in the solution by bubbles bursting at the surface of the suspension. For clean bubbles, the suspension is negatively charged with a zeta potential value of -41.4 ± 0.5 (Figure 3d), which would correspond to the zeta potential of all the cells (and of their excreted organic material) still in solution after flotation. Once the bubbles are coated with PO-chitosan, the global charge of the

solution shifts and becomes positive for all concentrations of PO-chitosan, with the highest value of 13.2 ± 3.8 mV obtained for a concentration of 25 mg/mL. In this case, as a large majority of cells have been removed, this value can be attributed to the residual PO-chitosan in the solution or to remaining cells perhaps coated with PO-chitosan. While the differences between the three concentrations tested are not significantly different, we can still observe that lower separation efficiencies correspond to a lower zeta potential that could be due to the presence of more negatively-charged cells in the solution after flotation. Altogether, these experiments then further prove that the separation efficiencies obtained with PO-chitosan bubbles are indeed due to the presence of the molecule on the surface of bubbles that allows the capture of the cells in the suspension.
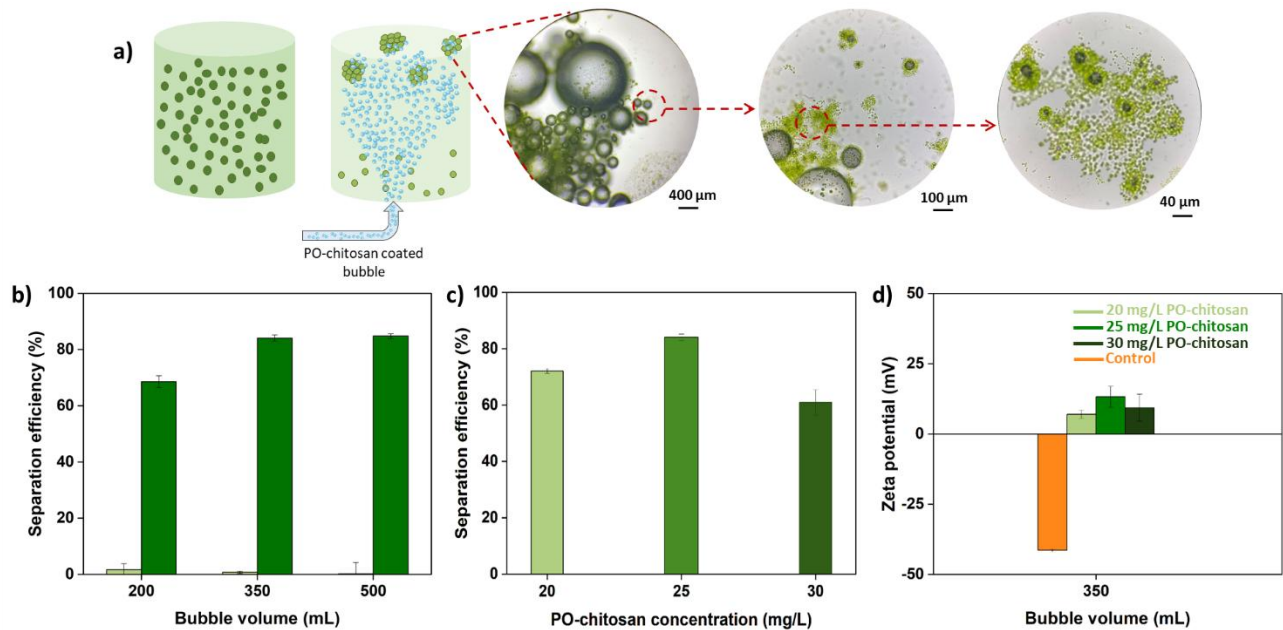

Figure 3: Flotation experiments of C. vulgaris strain F010102-A with PO-chitosan coated-bubble. a) Schematic representation of one-step flotation experiments and resulting optical images obtained from the top of the jar. b) Flotation efficiency of strain F010102-A cells with 25 mg/L PO-chitosan coated bubble with varying bubble volumes at no pH arrangement condition. Light green bars correspond to the control condition with clean bubbles, and dark green bars correspond to the test conditions with bubbles coated with PO-chitosan. c) Flotation efficiency of strain F010102-A cells at no pH arrangement condition with different PO-chitosan concentration of 20, 25 and 30 mg/L. d) corresponding zeta potential measurements of the suspension after flotation with clean bubble and PO-chitosan coated bubble at different concentrations and for a bubble volume of 350 mL.

These flotation results, while being very satisfactory, are also unexpected because of, as mentioned earlier, the low level of forces recorded in the case of the strain F010102-A cells with PO-functionalized bubbles. Compared to the CCAP strain, where much higher forces resulted in a maximum separation efficiency of 60%, it would have been expected here to obtain lower separation rates. Thus, another parameter must be involved, not present in the case of the CCAP strain. Such parameter could be the presence of AOM, *i. e.* a complex mixture of mostly exopolysaccharides and proteins that can be produced by cells during culture[41]. For instance, the team of Henderson hypothesized that the

separation efficiencies obtained using the PosiDAF process where bubbles are functionalized with positively-charged polymers, were influenced by AOM, which production and composition varies depending on the species considered[42]. To investigate this hypothesis, researchers eliminated AOM from the cell culture and performed flotation experiments using positively charged bubbles, revealing decreased separation efficiencies across all species. Moreover, substituting the AOM from a low-efficiency strain with that of a high-efficiency strain significantly enhanced separation efficiency, demonstrating the critical role of AOM in facilitating cell attachment to bubble surfaces[42]. These findings underscored the importance of AOM composition as a determining factor in bubble attachment. In our previous study, the removal of AOM from cells did not result in significant differences in the separation efficiencies obtained[20], most probably because the composition of the AOM excreted by the *C. vulgaris* strain CCAP could not mediate an attachment to the chitosan present at the surface of bubbles. To evaluate the potential role of AOM in the flotation of the strain F010102-A, we thus repeated the flotation experiments with the PO-chitosan bubbles with washed cells, for which AOM was removed. Note that in this case, we used a PO-chitosan concentration of 10 mg/mL to account for the lower concentration of cellular material in this case due to the removal of AOM. The separation efficiency decreased from 84.1 ± 1.1 % with AOM (Figure 3b and c) to 34.1% with washed cells, and the zeta potential of the cleared solution was of 15 ± 2.44 mV. This result suggests first that AOM is needed to promote the capture of cells by the functionalized bubbles, and second, that the AOM of the *C. vulgaris* strain F010102-A does interact with the chitosan at the surface of bubbles. Indeed, because the zeta potential is rather high although more cells remain in the solution, this means that a lot of bubbles rise without interacting with cells, burst at the surface, releasing the PO-chitosan in the underneath suspension, providing a global positive charge to the solution. Thus, this further comforts the hypothesis that AOM is an important factor in the interaction with PO-functionalized bubbles. Moreover, it is also in agreement with the results obtained by Henderson's team, but is also consistent with the low level of adhesion recorded between the cells and the functionalized bubbles (Figure 2b), which initially led to the assumption that lower separation efficiencies would be obtained than for the CCAP strain.

To prove this hypothesis and show the potential role of AOM in the attachment to bubbles, we then probed the interactions directly between isolated AOM and bubbles. For this, AOM was isolated from the culture medium of 6-days old cultures (mid-exponential phase) and immobilized on petri dishes. First of all, to verify the efficiency of this immobilization method and to verify the stability of AOM, we first recorded images of AOM using AFM in Quantitative Imaging mode. A 3D AFM height image of isolated AOM is presented in Figure 4a, and shows that the samples are indeed well immobilized on the surface, making it possible to probe their interactions with bubbles. For this, first, the interaction between clean bubbles and AOM were measured in force spectroscopy experiments. The results obtained (Figure 4b) show that AOM interacts with the bubble with multiple unbinding events visible on the retract force curves obtained. These unfoldings are associated to a maximum average adhesion force of 1.3 ± 0.6 nN (histogram in Figure 4b) and could be due to electrostatic interactions (bubble surface is negatively charged in water) between the bubbles and positive charges that may be present on AOM given its complex nature. To prove that these unfoldings do not simply come from the detachment of AOM from the surface they are immobilized on upon touching with the bubble probe, we also conducted control experiments where we measured first the interactions between AOM and the FluidFM probe without bubble (Figure S4a), and second the interactions between the FluidFM probe with no bubble and the petri-dish surface without AOM immobilized (Figure S4b). In the first case (AOM - FluidFM probe interactions), almost half of the retract force curves obtained present no retract peak

(inset in Figure S4a) and the ones that show interaction are lower in range (0.2 ± 0.2 nN) compared to the bubble-AOM interaction. Moreover, force signatures that are obtained are also different: in the case of FluidFM probe-AOM interaction, no multiple unbinding events were observed compared to AOM-bubble interactions (inset in Figure 4b). In the case of FluidFM cantilever and petri-dish interactions, force curves show a single peak happening at the contact point with an adhesion value of 66.3 ± 0.7 nN, typical of a hydrophobic interaction (Figure S4b). These additional experiments, together with the height image that could be generated of the AOM (Figure 4a) thus prove that AOM was correctly immobilized on the surface with the procedure used, allowing to confirm that indeed clean bubbles interact with AOM. But if these interactions between clean bubbles and cells were sufficient, separation would occur in flotation process with clean bubbles. Yet again, this is not the case, meaning that the functionalization of bubbles is essential to obtain an efficient separation of cells at the population scale. Moreover, as showed by measurements in Figure 3d, after flotation with clean bubbles (no separation at all), the remaining solution thus containing all the cells, is negative. Therefore, even if AOM interacts with bubbles in this case, because of the strong repulsion between cells and clean bubbles (Figure 1f), AOM might be in fact the only component removed from the water. To further understand if AOM plays a role in the flotation with functionalized bubbles, we then coated the bubble surface with PO-chitosan and directly measured their interaction with AOM. The results obtained are presented in Figure 4c, and show that AOM interacts with the PO-chitosan coated bubbles with multiple unbinding events visible on the retract force curves, most probably resulting this time from a specific interaction between the chitosan backbone at the surface of bubbles and polymers present in the AOM. These unfoldings are associated to an average adhesion force of 3.2 ± 0.1 nN, which represents a 2.5-fold increase compared to the force obtained with clean bubbles. These measurements thus prove that PO-chitosan bubbles are interacting not only with cells, but also with the AOM that cells produce. And as it was previously showed, AOM is a gel-like structure that bridges that can bridge cells together[43]. Further AFM imaging with unwashed cells (no AOM removal) in the case of this study was also performed, revealing indeed the formation of bridges arounds cells by the AOM present around them (Figure S5). Thus here, the following hypothesis can be formulated to explain the flotation results obtained. Indeed, while cells interact with PO-chitosan-bubbles with a low force level (300 pN), the AOM they produce can promote a much better attachment to bubbles (adhesion force increased by a factor of 10). And because AOM can also bridge the cells together, it acts as a carrier, resulting in high separation efficiency.
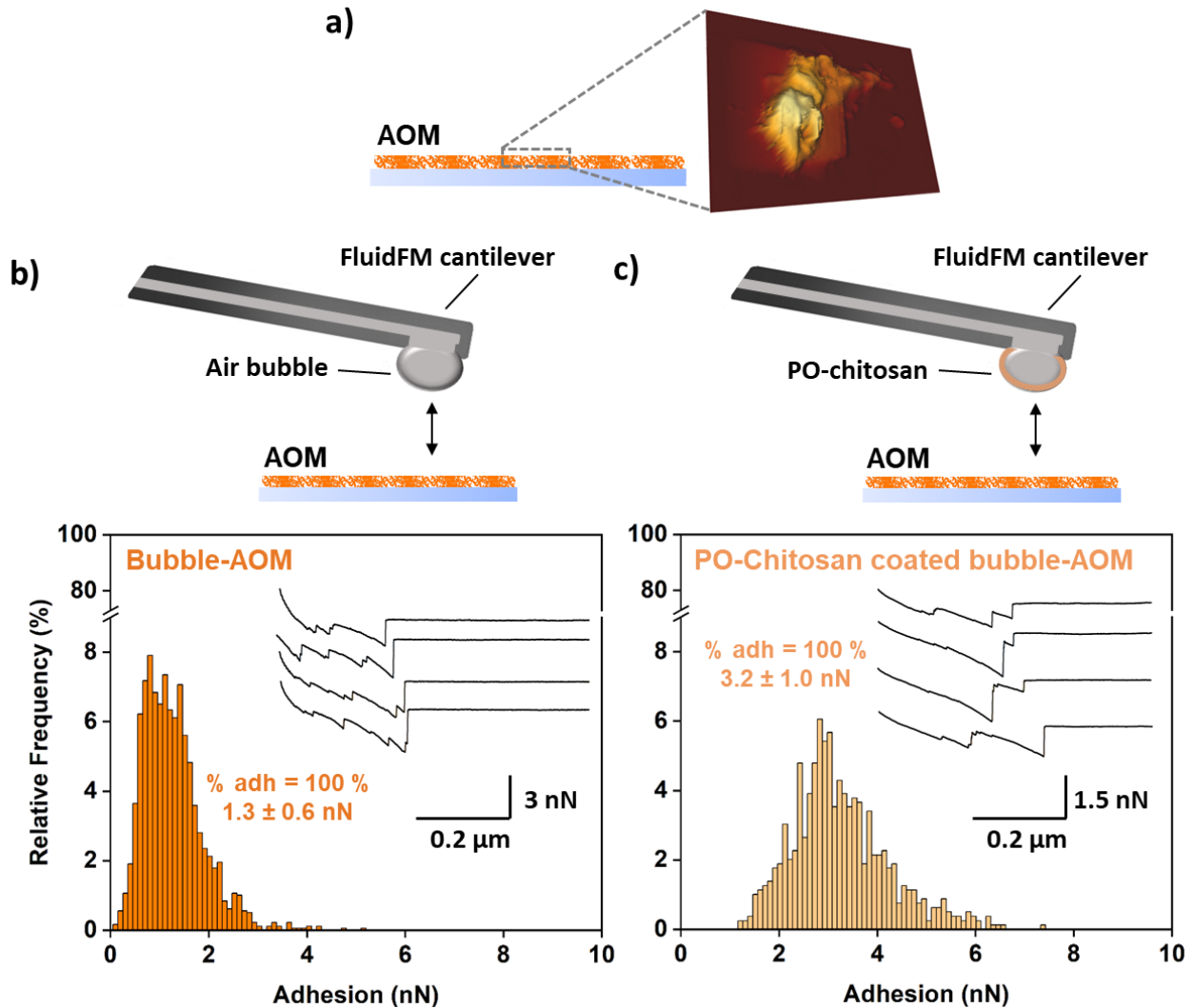
Figure 4. Interaction between single bubble and AOM. *a) 3D height images of AOM immobilized on petri dish (color-scale=3 µm, image of 25 x 25 µm). Schematic representation of the measurements performed and histogram showing the distributions of the adhesion forces recorded between b) clean bubbles and AOM immobilized on petri-dish surfaces and c) PO-chitosan coated bubble and AOM immobilized on petri-dish surfaces.*

PO-chitosan is an efficient flocculant at any pH for *C. vulgaris* strain F010102-A cells

With the comprehension of cell-PO-chitosan interactions in place, the final phase of this study involves evaluating the potential efficiency of this molecule as a flocculant. Contrary to the CCAP strain, the interactions between PO-chitosan and cells do not depend on hydrophobic interactions, but rather on specific ones, as explained before. However, what is important is that for the CCAP strain, the interaction was dependent on the pH because both the hydrophobicity of the cells surface and of the PO-chitosan molecule itself were also dependent on the pH. Yet, for the strain F010102-A cells, since the adhesion mechanism to PO-chitosan is different, based on specific interactions between the chitosan backbone of the molecules and cells, then it may be possible to get rid of the pH-dependency. To verify this point, we performed flocculation experiments with the *C. vulgaris* strain F010102-A cells using

different PO-chitosan concentrations at different pH values. The results are presented in Figure 5. Initially, the impact of varying PO-chitosan concentrations on flocculation was examined without altering the pH of the cell suspensions (measured at 8.2); the results are presented in Figure 5b. The flocculation efficiencies were of 0.0 ± 0.0 %, 94.9 ± 3.7 %, 98.4 ± 0.7% and 97.6 ± 0.9 % at PO-chitosan concentration of 0, 20,25 and 30 mg/L respectively. While all concentrations resulted in high separation rates, the highest flocculation efficiency of 98.4 ± 0.7 % was reached for 25 mg/L of PO-chitosan concentration which was chosen for the rest of the study. For *C. vulgaris* CCAP strain, the maximum flocculation efficiency was reached at a concentration of 30 mg/L of PO-chitosan, which is thus consistent [20]. However in that case, the flocculation efficiency decreased at higher pH (9), as both cells (*C. vulgaris* CCAP strain) and PO-chitosan were hydrophilic. Thus, in the next step, the effect of pH was investigated on PO-chitosan meditated flocculation with an optimized PO-chitosan concentration of 25 mg/L. The results obtained at pH 6, 7.4, 9 or at a non-adjusted pH (n.a.) conditions (ranging between 8 and 8.5) are presented in Figure 5c. At all pH values considered, the flocculation efficiencies are high; 97.7 ± 0.3 %, 95.5 ± 0.8 %, 98.0 ± 2.0 % and 98.4 ± 0.7 % at pH 6, 7.4, 9 and no arrangement (n.a.), respectively. This shows that PO-chitosan is efficient to flocculate strain F010102-A cells regardless of
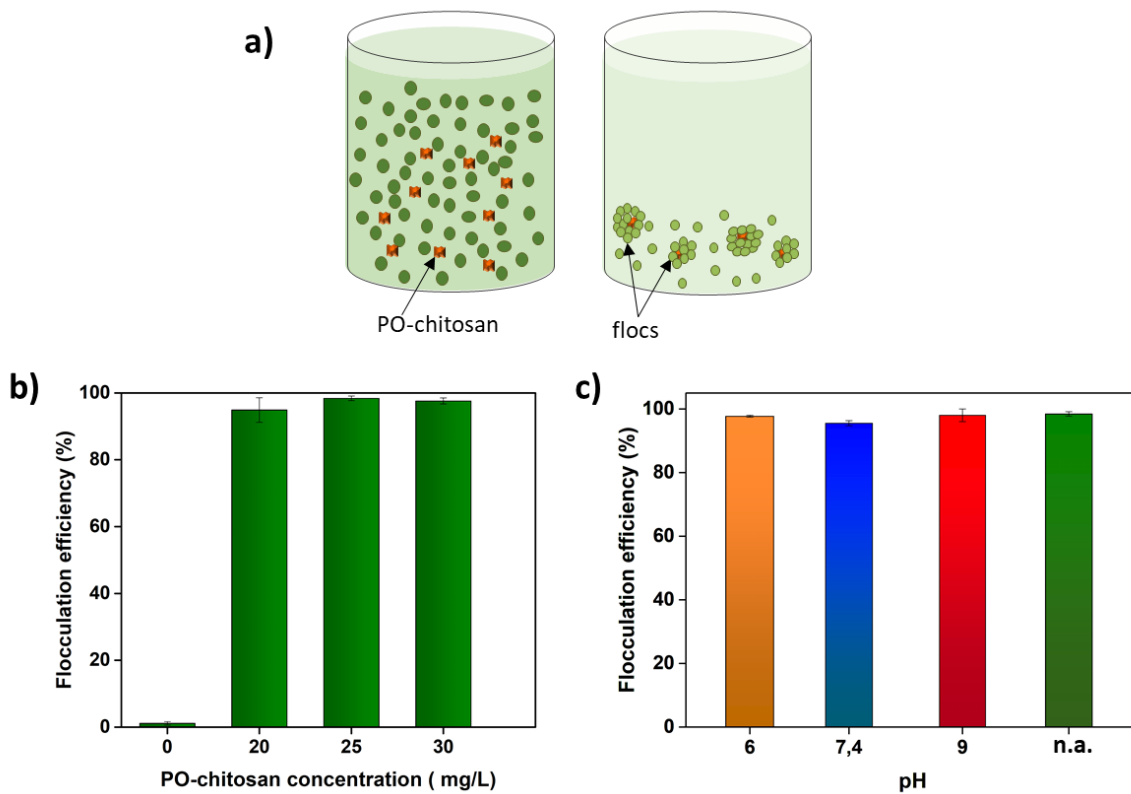
the pH.

Figure 5. PO-chitosan mediated flocculation experiments with C. vulgaris strain F010102-A cells a) Schematic representation of flocculation experiments. b) Flocculation efficiency with varying PO-chitosan concentrations of 0, 20, 25 and 30 mg/L at no pH arrangement condition. c) Flocculation efficiency of C. vulgaris strain F010102-A with 25 mg/L of PO-chitosan with varying pH.

Chitosan, increasingly utilized as a bio-based alternative to synthetic flocculants in wastewater treatment, is gaining popularity[16]. While effective in harvesting freshwater microalgae by generating large flocs at low doses (10-20 mg/L), chitosan necessitates a low pH to achieve higher separation yields[44,45,40,19,20]. For example, once the pH is increased from 6 to 7, which modifies the charge of chitosan (as the pKa of chitosan is 6.5), the required dose for maximum efficiency is increased. This is the case for example for the freshwater species *Chlorella sorokiniana*, where the chitosan dosage has to be increased from 5 to 10 mg/L with increasing pH [46], but it is also the case for *C. vulgaris* CCAP strain. In fact in this case, the adhesion mechanism between cells and chitosan is different depending on the pH; while at pH 6 it is based on specific interactions between chitosan and the cell wall of cells, at higher pH, chitosan precipitates and flocculates the cells through a sweeping mechanism, requiring in this case a higher dose of chitosan to induce a large enough precipitate to entrap all the cells present in the suspension [19]. For this species, PO-chitosan was already an interesting alternative, allowing to flocculate cells in wider pH ranges as long as both PO-chitosan and cell (*C. vulgaris CCAP strain*) were both hydrophobic (until pH 7.4, as detailed in [20]). But with the strain considered here, this hydrophobicity requirement is alleviated, and because PO-chitosan molecule does not precipitate at high pH like chitosan, then its use can be widened to any pH values. This is an important advantage as adjusting the pH of a microalgae culture at large scale can involve large amounts of acid and important mixing times.

CONCLUSIONS

In a previous study, our group had showed that an amphiphilic derivative of chitosan, PO-chitosan, could interact with *C. vulgaris* strain CCAP cells through hydrophobic interactions, allowing to separate cells efficiently using this molecule either as a flocculant or as a surfactant in flotation. Here in this work, we use a different *C. vulgaris* strain to evaluate if PO-chitosan could also be efficient to harvest cells with different cell surface properties. The first part of the work consisted in characterizing the surface properties of this new strain using AFM, which showed that cells of the strain F010102-A were indeed different, with a different cell wall composition as illustrated by nanomechanical properties. Yet the most important difference was the fact that cells are completely hydrophilic, raising the question if they would be able to interact with PO-chitosan at all. Force spectroscopy experiments then showed that despite being completely hydrophilic, *C. vulgaris* strain F010102-A cells were still able to interact with PO-chitosan bubbles through specific interactions and that no hydrophobic interactions was taking place in this case. However, adhesion force levels were rather low compared to those obtained with the CCAP strain (350 pN vs 13 nN), yet, flotation with functionalized bubbles resulted in better separation efficiencies, of 84% compared to 60% for the CCAP strain. To understand this, we investigated the role of AOM, and found that for strain F010102-A, the AOM produced during culture is in fact capable of interacting with PO-chitosan functionalized bubbles, and that removing it from the culture medium resulted in poor separation efficiencies. Thus, AOM in the experimental conditions used in this study could interact with the functionalized bubbles and act as a carrier by bridging the cells together during the flotation process. In addition, we found that because the interactions between PO-chitosan do not rely on hydrophobic interactions but rather on specific ones unlike for the CCAP strain, high separation efficiencies can also be achieved when using PO-chitosan as a flocculant independently of the pH, enlarging in a great manner the possible usage of this molecule. Altogether, these results show that despite different cell surface properties, flotation separation with functionalized bubbles can still be effective by relying on another mechanism. This shows the potential of this approach, which

could perhaps be used for other microalgae species, where different adhesion mechanisms could take place.

ACKNOWLEDGEMENTS

CONFLICTS OF INTEREST

The authors declare no conflicts of interest.

REFERENCES

(1) Barbosa, M. J.; Janssen, M.; Südfeld, C.; D'Adamo, S.; Wijffels, R. H. Hypes, Hopes, and the Way Forward for Microalgal Biotechnology. *Trends Biotechnol.* **2023**, *41* (3), 452–471. https://doi.org/10.1016/j.tibtech.2022.12.017.

(2) Brennan, L.; Owende, P. Biofuels from Microalgae—A Review of Technologies for Production, Processing, and Extractions of Biofuels and Co-Products. *Renew. Sustain. Energy Rev.* **2010**, *14* (2), 557–577. https://doi.org/10.1016/j.rser.2009.10.009.

(3) Dismukes, G. C.; Carrieri, D.; Bennette, N.; Ananyev, G. M.; Posewitz, M. C. Aquatic Phototrophs: Efficient Alternatives to Land-Based Crops for Biofuels. *Curr. Opin. Biotechnol.* **2008**, *19* (3), 235–240. https://doi.org/10.1016/j.copbio.2008.05.007.

(4) Rodolfi, L.; Zittelli, G. C.; Bassi, N.; Padovani, G.; Biondi, N.; Bonini, G.; Tredici, M. R. Microalgae for Oil: Strain Selection, Induction of Lipid Synthesis and Outdoor Mass Cultivation in a Low-Cost Photobioreactor. *Biotechnol. Bioeng.* **2009**, *102* (1), 100–112. https://doi.org/10.1002/bit.22033.

(5) Ziolkowska, J. R. Prospective Technologies, Feedstocks and Market Innovations for Ethanol and Biodiesel Production in the US. *Biotechnol. Rep.* **2014**, *4*, 94–98. https://doi.org/10.1016/j.btre.2014.09.001.

(6) Colling Klein, B.; Bonomi, A.; Maciel Filho, R. Integration of Microalgae Production with Industrial Biofuel Facilities: A Critical Review. *Renew. Sustain. Energy Rev.* **2018**, *82*, 1376–1392. https://doi.org/10.1016/j.rser.2017.04.063.

(7) Christenson, L.; Sims, R. Production and Harvesting of Microalgae for Wastewater Treatment, Biofuels, and Bioproducts. *Biotechnol. Adv.* **2011**, *29* (6), 686–702. https://doi.org/10.1016/j.biotechadv.2011.05.015.

(8) Lam, M. K.; Lee, K. T. Microalgae Biofuels: A Critical Review of Issues, Problems and the Way Forward. *Biotechnol. Adv.* **2012**, *30* (3), 673–690. https://doi.org/10.1016/j.biotechadv.2011.11.008.

(9)   Rashid, N.; Park, W.-K.; Selvaratnam, T. Binary Culture of Microalgae as an Integrated Approach for Enhanced Biomass and Metabolites Productivity, Wastewater Treatment, and Bioflocculation. *Chemosphere* **2018**, *194*, 67–75. https://doi.org/10.1016/j.chemosphere.2017.11.108.

(10) Tiron, O.; Bumbac, C.; Manea, E.; Stefanescu, M.; Nita Lazar, M. Overcoming Microalgae Harvesting Barrier by Activated Algae Granules. *Sci. Rep.* **2017**, *7* (1), 4646. https://doi.org/10.1038/s41598-017-05027-3.

(11) Laamanen, C. A.; Ross, G. M.; Scott, J. A. Flotation Harvesting of Microalgae. *Renew. Sustain. Energy Rev.* **2016**, *58*, 75–86. https://doi.org/10.1016/j.rser.2015.12.293.

(12) Molina Grima, E.; Belarbi, E.-H.; Acién Fernández, F. G.; Robles Medina, A.; Chisti, Y. Recovery of Microalgal Biomass and Metabolites: Process Options and Economics. *Biotechnol. Adv.* **2003**, *20* (7), 491–515. https://doi.org/10.1016/S0734-9750(02)00050-2.

(13) Lama, S.; Muylaert, K.; Karki, T. B.; Foubert, I.; Henderson, R. K.; Vandamme, D. Flocculation Properties of Several Microalgae and a Cyanobacterium Species during Ferric Chloride, Chitosan and Alkaline Flocculation. *Bioresour. Technol.* **2016**, *220*, 464–470. https://doi.org/10.1016/j.biortech.2016.08.080.

(14) Vandamme, D.; Foubert, I.; Muylaert, K. Flocculation as a Low-Cost Method for Harvesting Microalgae for Bulk Biomass Production. *Trends Biotechnol.* **2013**, *31* (4), 233–239. https://doi.org/10.1016/j.tibtech.2012.12.005.

(15) Pal, S.; Mal, D.; Singh, R. P. Cationic Starch: An Effective Flocculating Agent. *Carbohydr. Polym.* **2005**, *59* (4), 417–423. https://doi.org/10.1016/j.carbpol.2004.06.047.

(16) Renault, F.; Sancey, B.; Badot, P.-M.; Crini, G. Chitosan for Coagulation/Flocculation Processes – An Eco-Friendly Approach. *Eur. Polym. J.* **2009**, *45* (5), 1337–1348. https://doi.org/10.1016/j.eurpolymj.2008.12.027.

(17) Ritthidej, G. C. Chapter 3 - Nasal Delivery of Peptides and Proteins with Chitosan and Related Mucoadhesive Polymers. In *Peptide and Protein Delivery*; Van Der Walle, C., Ed.; Academic Press: Boston, 2011; pp 47–68. https://doi.org/10.1016/B978-0-12-384935-9.10003-3.

(18) Demir-Yilmaz, I.; Guiraud, P.; Formosa-Dague, C. The Contribution of Atomic Force Microscopy (AFM) in Microalgae Studies: A Review. *Algal Res.* **2021**, *60*, 102506. https://doi.org/10.1016/j.algal.2021.102506.

(19) Demir, I.; Blockx, J.; Dague, E.; Guiraud, P.; Thielemans, W.; Muylaert, K.; Formosa-Dague, C. Nanoscale Evidence Unravels Microalgae Flocculation Mechanism Induced by Chitosan. *ACS Appl. Bio Mater.* **2020**, *3* (12), 8446–8459. https://doi.org/10.1021/acsabm.0c00772.

(20) Demir-Yilmaz, I.; Ftouhi, M. S.; Balayssac, S.; Guiraud, P.; Coudret, C.; Formosa-Dague, C. Bubble Functionalization in Flotation Process Improve Microalgae Harvesting. *Chem. Eng. J.* **2023**, *452*, 139349. https://doi.org/10.1016/j.cej.2022.139349.

(21) Henderson, R. K.; Parsons, S. A.; Jefferson, B. Surfactants as Bubble Surface Modifiers in the Flotation of Algae: Dissolved Air Flotation That Utilizes a Chemically Modified Bubble Surface. *Environ. Sci. Technol.* **2008**, *42* (13), 4883–4888. https://doi.org/10.1021/es702649h.

(22) Henderson, R. K.; Parsons, S. A.; Jefferson, B. Polymers as Bubble Surface Modifiers in the Flotation of Algae. *Environ. Technol.* **2010**, *31* (7), 781–790. https://doi.org/10.1080/09593331003663302.

(23) Yap, R. K. L.; Rao, N. R. H.; Holmes, M.; Whittaker, M.; Stuetz, R. M.; Jefferson, B.; Bulmuş, V.; Peirson, W. L.; Henderson, R. K. Evaluating the Performance of Conventional DAF and PosiDAF Processes for Cyanobacteria Separation at a Pilot Plant Scale. *H2Open J.* **2022**, h2oj2022142. https://doi.org/10.2166/h2oj.2022.142.

(24) Meister, A.; Gabi, M.; Behr, P.; Studer, P.; Vörös, J.; Niedermann, P.; Bitterli, J.; Polesel-Maris, J.; Liley, M.; Heinzelmann, H.; Zambelli, T. FluidFM: Combining Atomic Force Microscopy and Nanofluidics in a Universal Liquid Delivery System for Single Cell Applications and Beyond. *Nano Lett.* **2009**, *9* (6), 2501–2507. https://doi.org/10.1021/nl901384x.

(25) Demir, I.; Lüchtefeld, I.; Lemen, C.; Dague, E.; Guiraud, P.; Zambelli, T.; Formosa-Dague, C. Probing the Interactions between Air Bubbles and (Bio)Interfaces at the Nanoscale Using FluidFM Technology. *J. Colloid Interface Sci.* **2021**, *604*, 785–797. https://doi.org/10.1016/j.jcis.2021.07.036.

(26) Gerken, H. G.; Donohoe, B.; Knoshaug, E. P. Enzymatic Cell Wall Degradation of Chlorella Vulgaris and Other Microalgae for Biofuels Production. *Planta* **2013**, *237* (1), 239–253. https://doi.org/10.1007/s00425-012-1765-0.

(27) Cheng, S.; Zhang, H.; Wang, H.; Mubashar, M.; Li, L.; Zhang, X. Influence of Algal Organic Matter in the In-Situ Flotation Removal of *Microcystis* Using Positively Charged Bubbles. *Bioresour. Technol.* **2024**, 130468. https://doi.org/10.1016/j.biortech.2024.130468.

(28) Silveira-Font, Y.; Gómez-Luna, L.; Kufundala-Wemba, M. D.; Salazar-Hernández, D.; Ortega-Díaz, Y. Variación de La Composición de Pigmentos de Chlorella Vulgaris Beijerinck, Con La Aplicación Del Campo Magnético Estático. *Rev. Cuba. Quím.* **2018**, *30* (1), 55–67.

(29) Demir-Yilmaz, I.; Yakovenko, N.; Roux, C.; Guiraud, P.; Collin, F.; Coudret, C.; ter Halle, A.; Formosa-Dague, C. The Role of Microplastics in Microalgae Cells Aggregation: A Study at the Molecular Scale Using Atomic Force Microscopy. *Sci. Total Environ.* **2022**, *832*, 155036. https://doi.org/10.1016/j.scitotenv.2022.155036.

(30) Hutter, J. L.; Bechhoefer, J. Calibration of Atomic-force Microscope Tips. *Rev. Sci. Instrum.* **1993**, *64* (7), 1868–1873. https://doi.org/10.1063/1.1143970.

(31) Rao, N. R. H.; Beyer, V. P.; Henderson, R. K.; Thielemans, W.; Muylaert, K. Microalgae Harvesting Using Flocculation and Dissolved Air Flotation: Selecting the Right Vessel for Lab-Scale Experiments. *Bioresour. Technol.* **2023**, *374*, 128786. https://doi.org/10.1016/j.biortech.2023.128786.

(32) Henderson, R. K.; Baker, A.; Parsons, S. A.; Jefferson, B. Characterisation of Algogenic Organic Matter Extracted from Cyanobacteria, Green Algae and Diatoms. *Water Res.* **2008**, *42* (13), 3435–3445. https://doi.org/10.1016/j.watres.2007.10.032.

(33) Li, H.; Li, Z.; Xiong, S.; Zhang, H.; Li, N.; Zhou, S.; Liu, Y.; Huang, Z. Pilot-Scale Isolation of Bioactive Extracellular Polymeric Substances from Cell-Free Media of Mass Microalgal Cultures Using Tangential-Flow Ultrafiltration. *Process Biochem.* **2011**, *46* (5), 1104–1109. https://doi.org/10.1016/j.procbio.2011.01.028.

(34) Gaignard, C.; Laroche, C.; Pierre, G.; Dubessay, P.; Delattre, C.; Gardarin, C.; Gourvil, P.; Probert, I.; Dubuffet, A.; Michaud, P. Screening of Marine Microalgae: Investigation of New Exopolysaccharide Producers. *Algal Res.* **2019**, *44*, 101711. https://doi.org/10.1016/j.algal.2019.101711.

(35) Villacorte, L. O.; Ekowati, Y.; Neu, T. R.; Kleijn, J. M.; Winters, H.; Amy, G.; Schippers, J. C.; Kennedy, M. D. Characterisation of Algal Organic Matter Produced by Bloom-Forming Marine and Freshwater Algae. *Water Res.* **2015**, *73*, 216–230. https://doi.org/10.1016/j.watres.2015.01.028.

(36) Demir-Yilmaz, I.; Schiavone, M.; Esvan, J.; Guiraud, P.; Formosa-Dague, C. Combining AFM, XPS and Chemical Hydrolysis to Understand the Complexity and Dynamics of C. Vulgaris Cell Wall Composition and Architecture. *Algal Res.* **2023**, *72*, 103102. https://doi.org/10.1016/j.algal.2023.103102.

(37) Formosa-Dague, C.; Feuillie, C.; Beaussart, A.; Derclaye, S.; Kuchaříková, S.; Lasa, I.; Van Dijck, P.; Dufrêne, Y. F. Sticky Matrix: Adhesion Mechanism of the Staphylococcal Polysaccharide Intercellular Adhesin. *ACS Nano* **2016**, *10* (3), 3443–3452. https://doi.org/10.1021/acsnano.5b07515.

(38) Higgins, M. J.; Molino, P.; Mulvaney, P.; Wetherbee, R. The Structure and Nanomechanical Properties of the Adhesive Mucilage That Mediates Diatom-Substratum Adhesion and Motility1. *J. Phycol.* **2003**, *39* (6), 1181–1193. https://doi.org/10.1111/j.0022-3646.2003.03-027.x.

(39) Yang, C.; Dabros, T.; Li, D.; Czarnecki, J.; Masliyah, J. H. Measurement of the Zeta Potential of Gas Bubbles in Aqueous Solutions by Microelectrophoresis Method. *J. Colloid Interface Sci.* **2001**, *243* (1), 128–135. https://doi.org/10.1006/jcis.2001.7842.

(40) Blockx, J.; Verfaillie, A.; Thielemans, W.; Muylaert, K. Unravelling the Mechanism of Chitosan-Driven Flocculation of Microalgae in Seawater as a Function of pH. *ACS Sustain. Chem. Eng.* **2018**, *6* (9), 11273–11279. https://doi.org/10.1021/acssuschemeng.7b04802.

(41) Nagar, S.; Antony, R.; Thamban, M. Extracellular Polymeric Substances in Antarctic Environments: A Review of Their Ecological Roles and Impact on Glacier Biogeochemical Cycles. *Polar Sci.* **2021**, *30*, 100686. https://doi.org/10.1016/j.polar.2021.100686.

(42) Hanumanth Rao, N. R.; Yap, R.; Whittaker, M.; Stuetz, R. M.; Jefferson, B.; Peirson, W. L.; Granville, A. M.; Henderson, R. K. The Role of Algal Organic Matter in the Separation of Algae and Cyanobacteria Using the Novel "Posi" - Dissolved Air Flotation Process. *Water Res.* **2018**, *130*, 20–30. https://doi.org/10.1016/j.watres.2017.11.049.

(43) Vergnes, J. B.; Gernigon, V.; Guiraud, P.; Formosa-Dague, C. Bicarbonate Concentration Induces Production of Exopolysaccharides by Arthrospira Platensis That Mediate Bioflocculation and Enhance Flotation Harvesting Efficiency. *ACS Sustain. Chem. Eng.* **2019**, *7* (16), 13796–13804. https://doi.org/10.1021/acssuschemeng.9b01591.

(44) Divakaran, R.; Sivasankara Pillai, V. N. Flocculation of Algae Using Chitosan. *J. Appl. Phycol.* **2002**, *14* (5), 419–422. https://doi.org/10.1023/A:1022137023257.

(45) Ahmad, A. L.; Mat Yasin, N. H.; Derek, C. J. C.; Lim, J. K. Optimization of Microalgae Coagulation Process Using Chitosan. *Chem. Eng. J.* **2011**, *173* (3), 879–882. https://doi.org/10.1016/j.cej.2011.07.070.

(46) Xu, Y.; Purton, S.; Baganz, F. Chitosan Flocculation to Aid the Harvesting of the Microalga Chlorella Sorokiniana. *Bioresour. Technol.* **2013**, *129*, 296–301. https://doi.org/10.1016/j.biortech.2012.11.068.